JACS
JOURNAL OF THE AMERICAN CHEMICAL SOCIETY

ARTICLE

pubs.acs.org/JACS

Stepwise Effective Molarities in Porphyrin Oligomer Complexes: Preorganization Results in Exceptionally Strong Chelate Cooperativity

Hannah J. Hogben, Johannes K. Sprafke, Markus Hoffmann, Miłosz Pawlicki, and Harry L. Anderson*

Department of Chemistry, University of Oxford, Chemistry Research Laboratory, Mansfield Road, Oxford OX1 3TA, United Kingdom

Supporting Information

ABSTRACT: Complexes of zinc porphyrin oligomers with multivalent ligands can be denatured by adding a large excess of a monodentate ligand, such as quinuclidine. We have used denaturation titrations to determine the stabilities of the complexes of a cyclic zinc−porphyrin hexamer with multidentate ligands with two to six pyridyl coordination sites. The corresponding complexes of linear porphyrin oligomers were also investigated. The results reveal that the stepwise effective molarities (EMs) for the third through sixth intramolecular coordination events with the cyclic hexamer are extremely high (EM = 10^2−10^3 M), whereas the values for the linear porphyrin oligomers are modest (EM ≈ 0.05 M). The speciation profiles for the denaturation reactions demonstrate that intermediate species are not significantly populated and that these equilibria are well described by a highly cooperative two-state model.

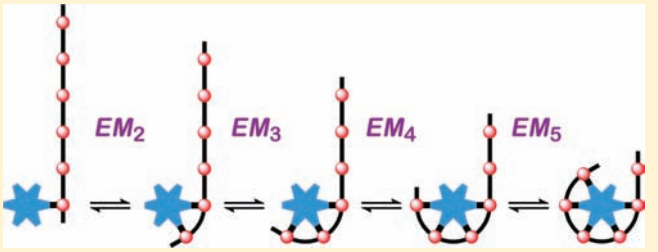

INTRODUCTION

When two molecules bind noncovalently through more than one point of interaction, the overall thermodynamic stability of the resulting complex can be substantially greater than would result from a single-point interaction.[1−3] This principle of multivalency underlies all biological molecular recognition and supramolecular self-assembly. The synergy between interactions which causes the increased stability of closed multivalent complexes is called "chelate cooperativity".[2,3a] It originates from the chelate effect, and it can be attributed to the fact that intermolecular interactions require an extra loss of translational and rotational entropy when compared with intramolecular interactions. A key parameter for quantifying the chelate cooperativity between two interactions is the effective molarity, EM, which is just the equilibrium constant for forming the chelated complex (K_{chel}) divided by the product of the two single-site binding constants (K_AK_B), as illustrated in Figure 1 and the following equation:[1,2,4]

$$\mathrm{EM} = \frac{K_{chel}}{K_AK_B} \qquad (1)$$

In practice, the value of EM is difficult to predict or calculate (except in the case of cyclization of a completely flexible chain, when EM ∝ $i^{-3/2}$, where i is the number of segments in the chain).[5−10] This problem is a serious obstacle to predicting the stability of noncovalent complexes.

The principle of preorganization, pioneered by Cram in the early 1980s,[11] states that EM can be maximized by designing a receptor with a well-defined shape, so that it is locked in the correct conformation for binding. This concept has had a huge influence on the design of synthetic receptors;[12] however, recently, several authors have questioned whether too much emphasis is placed on the use of rigid preorganized structures for molecular recognition. It has been suggested that the effort required to create a rigid receptor is often not sufficiently rewarded by high binding constants, that values of EM for supramolecular systems rarely exceed about 1 M, and that these modest effective molarities can be achieved using flexible host−guest systems, which are easier to synthesize.[7,10,13] Here we show that rigid preorganized host and guest structures can achieve EM values which greatly exceed those encountered in flexible systems, even when the binding sites are many atoms apart.

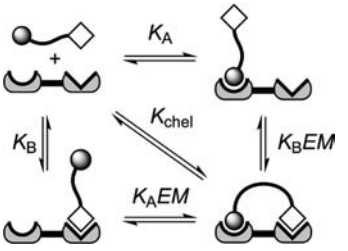

Figure 1. Formation of a chelated complex between two two-site species illustrates the definition of effective molarity, EM. This analysis assumes that the binding sites act independently when they bind monodentate ligands, i.e., that the system does not exhibit allosteric cooperativity.[4]

The chelate effect was discovered in the context of the coordination of diamines, such as 1,2-diaminoethane, to metal cations. Bidentate ligands typically bind metal ions more strongly

Received: October 1, 2011
Published: November 17, 2011

Chart 1. Structures of the Complexes Investigated during This Study[a]

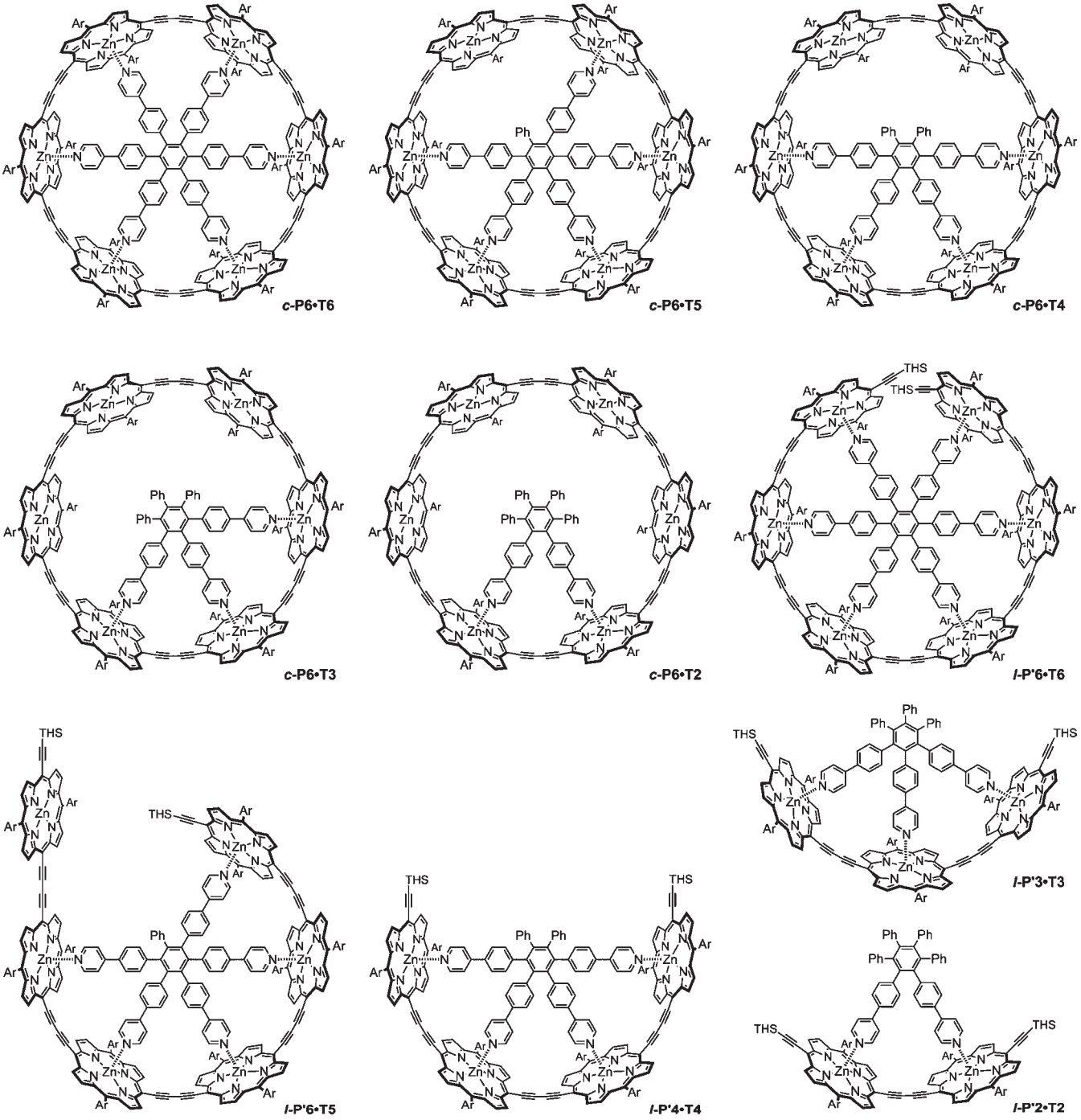

[a]See the stability constants in Table 1. Ar is 3,5-di-*tert*-butylphenyl in *c*-P6 and 3,5-bis(octyloxy)phenyl in *l*-P′2, *l*-P′3, *l*-P′4, and *l*-P′6. THS is $Si(C_6H_{13})_3$.

than the corresponding monodentate ligands by a factor of EM ≈ 50−100 M.[14] The equilibrium for dehydration of succinic acid to succinic anhydride is more favorable than the corresponding process for acetic acid by a factor of EM ≈ 10^5 M,[1] and the formation of cyclic disulfides exhibits chelate effects of up to EM ≈ 10^3 M.[15] However, these equilibria involve formation of covalent five- and six-membered rings. Larger ring sizes are generally associated with much lower effective molarities, and most supramolecular multivalent systems display thermodynamic effective molarities in the range of 0.01−10 M.[3c,6−10,16−24] Here we analyze a supramolecular system exhibiting effective molarities of up to about 10^3 M. Recently, we reported that the cyclic zinc porphyrin hexamer *c*-P6 forms an exceptionally stable 1:1 complex with the hexapyridyl template T6.[25,26] Here we present a detailed analysis of this binding process. By comparing the stability constants of the 1:1 complexes of ligands featuring

dx.doi.org/10.1021/ja209254r |*J. Am. Chem. Soc.* 2011, 133, 20962–20969

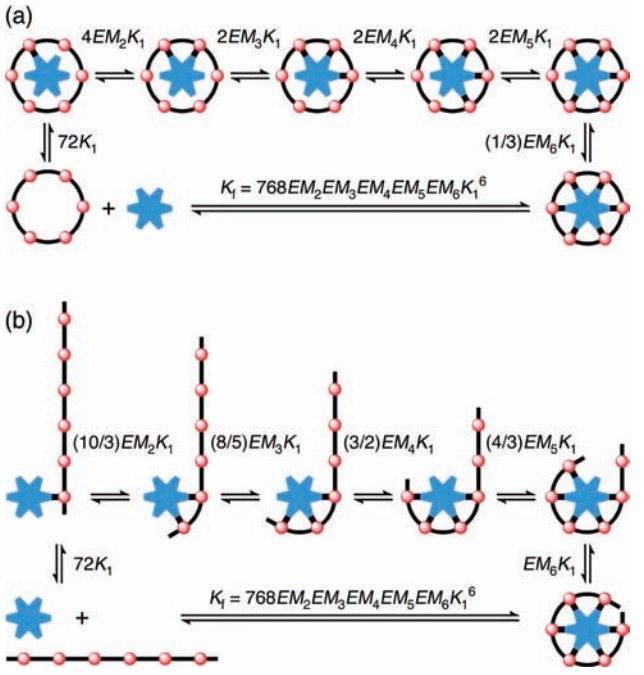

Figure 2. Stepwise equilibria defining the effective molarities EM_2–EM_6 (a) for formation of *c*-P6·T6 and (b) for formation of *l*-P′6·T6. K_1 is the microscopic binding constant for coordination of a pyridyl group to one face of a zinc site. For simplicity, isomers of intermediate complexes are not shown, but their formation is taken into account by the statistical factors. (See the Supporting Information for calculation of the statistical factors.)

two to six binding sites, T2, T3, T4, T5, and T6, with both cyclic hexamer *c*-P6 and linear oligomers *l*-P′2, *l*-P′3, *l*-P′4, and *l*-P′6 (Chart 1), we have determined the individual stepwise effective molarities for coordination of the second, third, fourth, fifth, and sixth site of the template, EM_2–EM_6 (Figure 2). The *c*-P6/T6 system is highly preorganized and has excellent geometrical complementarity,[26] resulting in very high EM values and an overall 1:1 association constant of 10^{36} M^{-1}, which is beyond the range of those of previously studied supramolecular systems.[27] In contrast, the linear hexamer *l*-P′6 is less well preorganized for binding these ligands, and its effective molarities, EM_2–EM_6, are all around 0.05 M.

RESULTS

Synthesis. Ligands T2–T5 were synthesized using the modular approach outlined in Scheme 1. Aldol condensation of a benzil derivative (blue) with a ketone (black) gave a tetracyclone that was converted to the corresponding ligand by Diels–Alder cyclization with a tolan derivative (red) (see the Supporting Information for experimental details).[28] Ligand T6, porphyrin nanoring *c*-P6, and the linear porphyrin oligomers *l*-P′*N* (*N* = 1, 2, 3, 4, and 6) were synthesized as reported previously.[25,26,29]

UV/Vis Titrations. The 1:1 complexes shown in Chart 1 were generated by titrating solutions of the porphyrin oligomers in chloroform with the ligands T*N*. These UV/vis titrations gave sharp end points (see the Supporting Information), but the complexes are mostly too stable ($K_f > 10^8$ M^{-1}) for their association constants to be determined from their formation curves. Thus, denaturation was used to determine K_f indirectly via the denaturation constant K_{dn}. A large excess of quinuclidine was titrated into solutions of the 1:1 complex (ca. 10^{-6} M in $CHCl_3$ at 298 K) to displace the multidentate ligands (Figure 4). For example, in the denaturation of *c*-P6·T*N*, K_{dn} is defined by eq 2, where [Q] is the concentration of quinuclidine. The corresponding binding isotherm is given by eq 3

Scheme 1. Synthesis of Ligands T2–T5

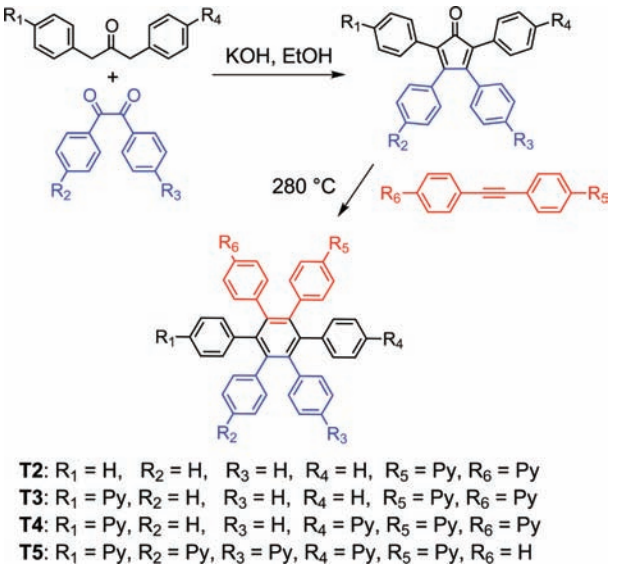

$$K_{dn} = \frac{[c\text{-P6}\cdot Q_6][TN]}{[c\text{-P6}\cdot TN][Q]^N} \quad (2)$$

$$\frac{A - A_0}{A_f - A_0} = \frac{-K_{dn}[Q]^N + \sqrt{K_{dn}{}^2[Q]^{2N} + 4K_{dn}[Q]^N[P]_0}}{2[P]_0} \quad (3)$$

where A is the absorption at a given point in the titration, A_0 is the initial absorption at [Q] = 0, A_f is the asymptotic final absorption at [Q] = ∞, and $[P]_0$ is the total concentration of 1:1 porphyrin oligomer template complex at the start of the titration. Binding isotherms derived from changes in absorption at selected wavelengths were analyzed by simulation with eq 3 to give the smooth curves plotted in Figure 4, with just three free parameters (A_0, A_f, and K_{dn}).

The derivation of eq 3 assumes that the concentration of free quinuclidine [Q] can be approximated to the total concentration of quinuclidine, which is valid since $[Q] \gg [P]_0$ throughout the fitted regions of the denaturation curves. Our analysis also assumes that the denaturation processes are essentially all-or-nothing two-state equilibria (i.e., that intermediate partially denatured species do not build up to high concentrations). This assumption is supported by the isosbestic nature of the UV/vis titrations (Figure 4) and by the good fits of this simple model to the experimental isotherms. The calculated speciation profiles also confirm that a two-state model is consistent with the results (see the Discussion). The resulting values of K_{dn} are listed in Table 1.

Denaturation constants were used to calculate the formation constants K_f via the thermodynamic cycle shown in Figure 3 using the following equation:

$$K_f = \frac{K_Q{}^N}{K_{dn}} \quad (4)$$

Table 1. Equilibrium Constants for the Porphyrin Oligomer Complexes Shown in Chart 1[a]

N	complex	K_{dn}	log K_f	K_σ	log $K_{chem,N}$	log $\overline{EM}_N$	log EM_N
2	*l*-P′2·T2	$(4.4 \pm 1.3) \times 10^4$ M^{-1}	7.5 ± 0.2	8	6.6 ± 0.2	-1.3 ± 0.3	-1.3 ± 0.3
3	*l*-P′3·T3	$(6.3 \pm 1.9) \times 10^7$ M^{-2}	10.4 ± 0.3	16	9.2 ± 0.3	-1.3 ± 0.2	-1.4 ± 0.2
4	*l*-P′4·T4	$(6.0 \pm 1.8) \times 10^{10}$ M^{-3}	13.5 ± 0.4	32	12.0 ± 0.4	-1.3 ± 0.2	-1.2 ± 0.2
5	*l*-P′6·T5	$(3.1 \pm 0.9) \times 10^{13}$ M^{-4}	16.9 ± 0.5	128	14.8 ± 0.5	-1.3 ± 0.2	-1.2 ± 0.2
6	*l*-P′6·T6	$(2.5 \pm 0.8) \times 10^{16}$ M^{-5}	20.1 ± 0.5	768	17.2 ± 0.5	-1.3 ± 0.2	-1.6 ± 0.2
2	*c*-P6·T2	(570 ± 170) M^{-1}	8.4 ± 0.2	48	6.8 ± 0.2	-0.81 ± 0.3	-0.81 ± 0.3
3	*c*-P6·T3	(14 ± 4) M^{-2}	15.6 ± 0.3	96	13.6 ± 0.3	1.2 ± 0.2	3.1 ± 0.2
4	*c*-P6·T4	(1.2 ± 0.4) M^{-3}	22.3 ± 0.4	192	20.0 ± 0.4	1.6 ± 0.2	2.6 ± 0.2
5	*c*-P6·T5	$(2.3 \pm 0.7) \times 10^{-2}$ M^{-4}	29.6 ± 0.5	384	27.0 ± 0.5	2.0 ± 0.2	3.2 ± 0.2
6	*c*-P6·T6	$(2.7 \pm 0.8) \times 10^{-3}$ M^{-5}	36.1 ± 0.5	768	33.2 ± 0.5	2.1 ± 0.2	2.4 ± 0.2

[a] Errors estimated from at least two replicates. See the Supporting Information for calculation of K_σ. Logarithms are decadic.

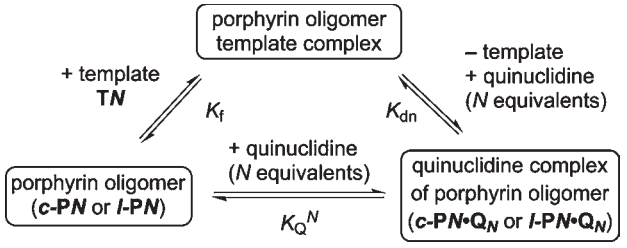

Figure 3. Thermodynamic cycle relating the formation constant of the template complex (K_f) to the denaturation constant (K_{dn}) and binding constant of each porphyrin unit for quinuclidine (K_Q).

The reference constant K_Q was approximated to the binding constant for coordination of quinuclidine to porphyrin monomer *l*-P′1 ($K_Q = 1.2 \times 10^6$ M^{-1}) for the linear oligomer complexes and coordination of quinuclidine to cyclic hexamer *c*-P6 ($K_Q = 3.6 \times 10^5$ M^{-1}) for the cyclic complexes.[30] Figure 4 shows that the absorption spectra of the complexes with multidentate ligands are generally red-shifted and more structured compared to the quinuclidine-bound oligomers at the end of the titration due to the more rigid structures and reduced porphyrin−porphyrin dihedral angles in the template complexes.[31,32] The denaturation curves become increasingly sigmoidal and cooperative as the number of coordination sites increases for both linear and cyclic complexes. The change in the shape of the UV/vis spectra during denaturation is most dramatic with the linear porphyrin oligomers (Figure 4a−e) due to the greater change in conformation compared with that of the preorganized cyclic hexamer (Figure 4f−j).

Statistical Factors. To understand the stability constants of different complexes, it is useful to factor out statistical contributions.[33] Thus, a measured equilibrium constant K_{eq} can be factorized into its statistical component K_σ and its statistically corrected value K_{chem} according to eq 5,[34] where for each species i, Q_i is the partition coefficient, Q'_i is the statistically corrected partition coefficient, and σ_i is the symmetry number. In Table 1, K_f is the measured formation constant from eq 4, K_σ is the corresponding statistical factor from eq 5 (see the Supporting Information for details), and $K_{chem,N}$ is the statistically corrected value of K_f.

$$wA + xB \overset{K_{eq}}{\rightleftharpoons} yC + zD$$

$$K_{eq} = \frac{Q_C{}^y Q_D{}^z}{Q_A{}^w Q_B{}^x} = \frac{Q_A{}^w Q_B{}^x}{Q_C{}^y Q_D{}^z} \frac{Q'_C{}^y Q'_D{}^z}{Q'_A{}^w Q'_B{}^x} = K_\sigma K_{chem} \quad (5)$$

Effective Molarities. Consideration of the thermodynamic cycles in Figure 2 shows that $K_{chem,N}$ for a system with N interactions is the product of $N - 1$ effective molarities, as expressed by the following equation:[35]

$$K_{chem,N} = K_1{}^N \prod_{m=2}^{m=N} EM_m \quad (6)$$

The stepwise effective molarities for the Nth interaction EM_N can thus be calculated using the following equation:

$$EM_N = \frac{K_{chem,N}}{K_{chem,N-1} K_1} \quad (7)$$

The geometric average of all the effective molarities contributing to the stability constant of a complex with N interactions is defined by eq 8 and calculated by eq 9.

$$\overline{EM}_N = \sqrt[N-1]{\prod_{m=2}^{m=N} EM_m} \quad (8)$$

$$\overline{EM}_N = \sqrt[N-1]{\frac{K_{chem,N}}{K_1{}^N}} \quad (9)$$

The K_1 in eqs 6−9 and Figure 2 is a reference single-site microscopic binding constant (statistically corrected for binding to one face of a porphyrin monomer). We estimated K_1 using the binding of 4-phenylpyridine to the porphyrin monomer *l*-P′1 ($K_1 = 1.0 \times 10^4$ M^{-1}) for the linear oligomers and to cyclic hexamer *c*-P6 ($K_1 = 6.0 \times 10^3$ M^{-1}) for the cyclic complexes. Values of K_f, K_{chem}, $\overline{EM}_N$, and EM_N are listed in Table 1 as decadic logarithms. The effective molarities have significant uncertainties because each value of EM is calculated from four experimentally determined binding constants ($K_{dn,N}$, $K_{dn,N-1}$, K_1, and K_Q).

DISCUSSION

The stepwise effective molarities EM_N for binding the linear oligomers *l*-P′N are small and show little variation from EM_2 to EM_6 (range 0.03−0.07 M; Figure 5a, green curve); thus, the average effective molarities $\overline{EM}_N$ for these linear systems are essentially independent of N (range 0.04−0.05 M; Figure 5b). The first effective molarity for *c*-P6 is also low (EM_2 = 0.15 M),

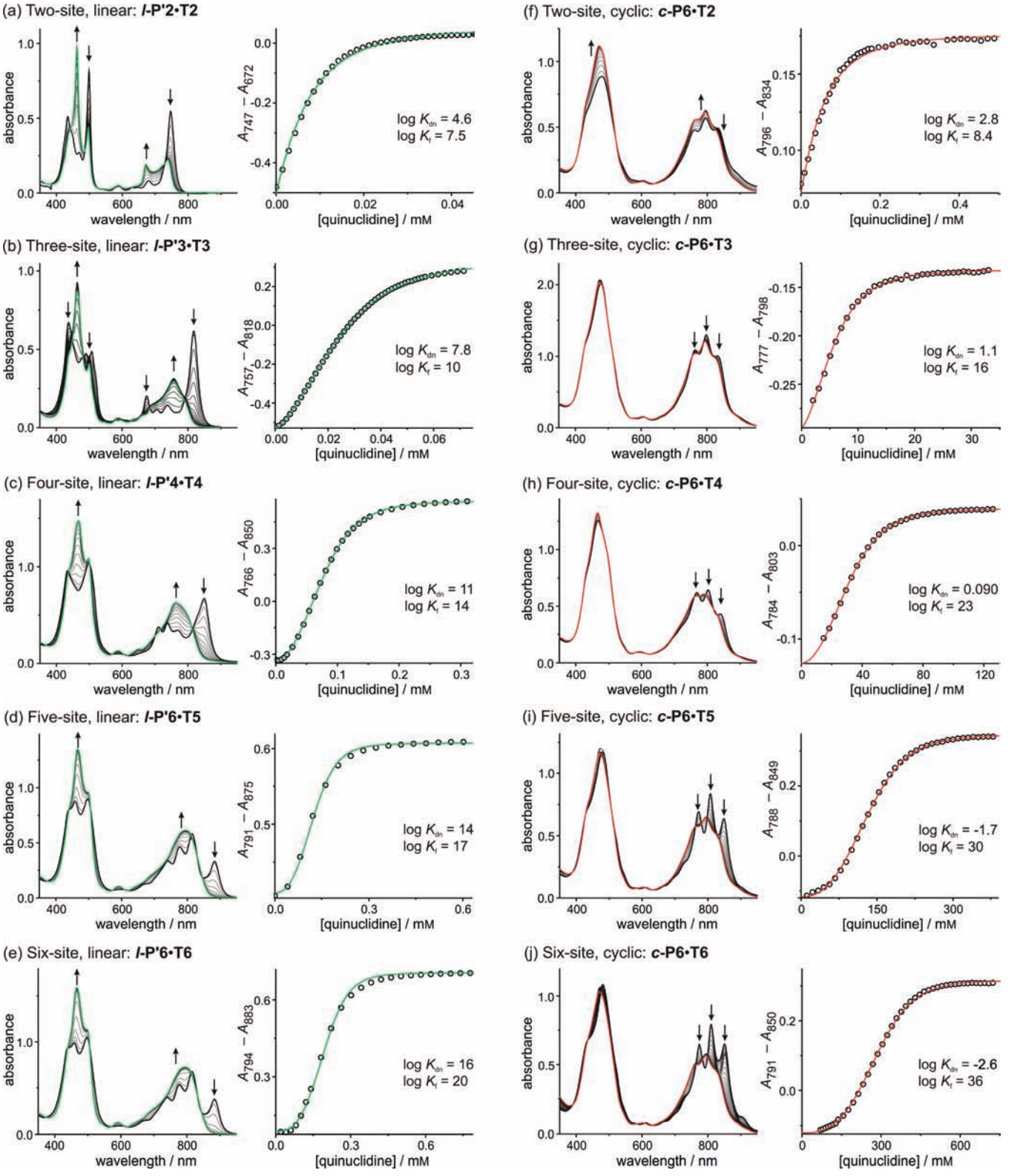

Figure 4. UV/vis denaturation titrations of linear (a−e, green) and cyclic (f−j, red) complexes (all in $CHCl_3$ at 298 K). The spectra are shown on the left with the spectra of the complexes in thick black lines and the end spectra (of the quinuclidine-saturated oligomers) in green (linear) and red (cyclic) lines. On the right are shown the experimental (black circles) and calculated (colored lines) binding isotherms, fitted to eq 3.

but the following effective molarities EM_3−EM_6 are several orders of magnitude larger (range 280−1700 M; Figure 5a, red curve). The variation in the values of EM_3−EM_6 is comparable with the experimental error, while the average effective molarities $\overline{EM}_N$ increase from $\overline{EM}_3$ to $\overline{EM}_6$ due the decreasing contribution from EM_2.

dx.doi.org/10.1021/ja209254r |J. Am. Chem. Soc. 2011, 133, 20962–20969

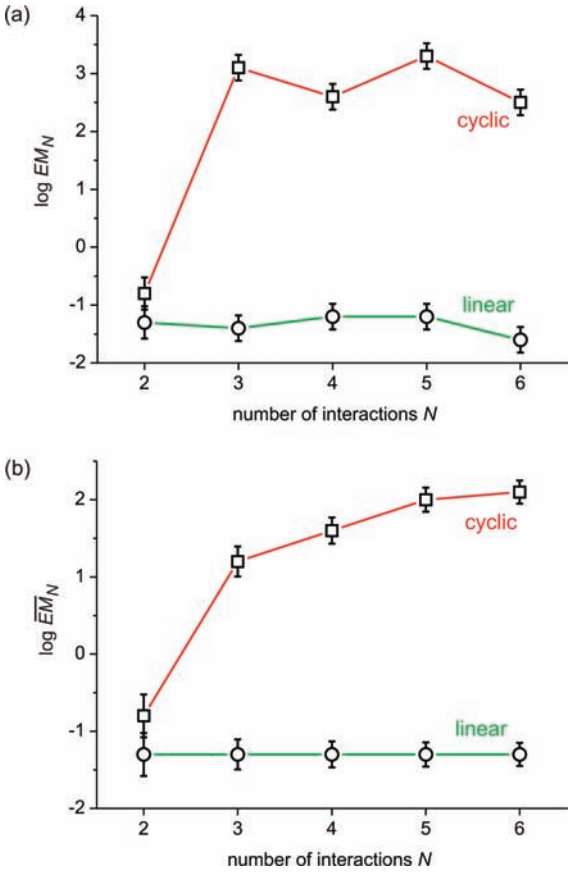

Figure 5. Stepwise (a) and geometric average (b) effective molarities for formation of linear (black circles, green lines) and cyclic (black squares, red lines) complexes as a function of N. Red and green lines are guides to the eye.

The high effective molarities exhibited by the cyclic hexamer, compared to the linear oligomers, reflect enthalpic and entropic preoganization. Butadiyne-linked porphyrin oligomers *l*-P′N are shape-persistent rods, and the length of linear hexamer *l*-P′6 (ca. 7 nm) is well below the persistence length (ca. 19 nm),[36,37] so there must be a significant enthalpy cost associated with bending this molecule into a cyclic conformation, whereas the geometry of *c*-P6 is almost ideal for binding T6.[26] According to Ercolani's terminology, formation of the complexes *c*-P6·TN, in contrast to formation of the complexes of the linear oligomers, displays interannular cooperativity.[3a]

It is surprising that EM_2 for *c*-P6 is only about 3 times larger than EM_2 for *l*-P′2. This probably reflects the significant loss of entropy on formation of the second bond in the cyclic complex; while formation of the first bond could occur inside or outside the nanoring, the second binding event can only occur inside the cavity. For subsequent coordination events, the ligand is fixed in place and the advantage of preorganization is maximized.

For the cyclic hexamer *c*-P6, the ratio EM_3/EM_2 is 8800. This corresponds to a huge increase in ligand affinity after the second zinc−pyridyl bond has been formed. The intermediate with two zinc−pyridyl interactions must be particularly rigid, so that little entropy is lost on formation of a third zinc−ligand bond, and this factor of about 10^4 is too large to arise from restricted rotation about a single bond.[10,38] The formation of two zinc−nitrogen interactions probably increases the rigidity of the host by preventing rotation of the porphyrins about the acetylene links, by preventing rotation of the bound guest, and by preventing low-frequency vibrations; changes in solvation may also make an important contribution.

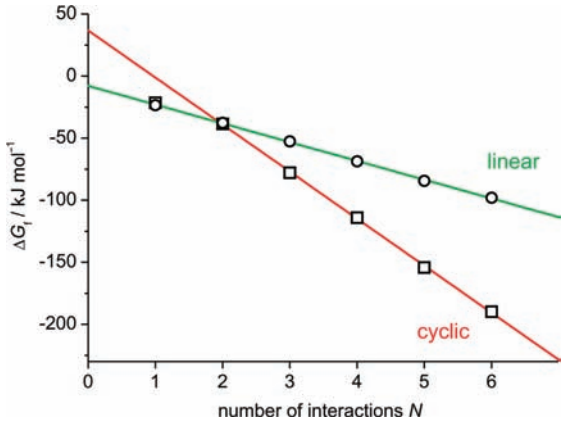

Figure 6. Gibbs free energies of complex formation of linear (black circles) and cyclic (black squares) complexes as a function of the number of interactions N. The error bars are smaller than the data points and thus are not shown. Linear fits to the data are shown as a green and a red line for linear and cyclic complexes, respectively.

The statistically corrected Gibbs free energy of complex formation ΔG_f increases linearly with the number of interactions N for the linear oligomers (Figure 6). For the cyclic hexamer complexes, ΔG_f increases more steeply after a discontinuity at $N = 2$. This discontinuity reflects the dramatic increase in EM in *c*-P6 when $N > 2$. These plots of ΔG_f against N provide an alternative approach to estimating the geometrical average effective molarities by the following equation:

$$\begin{aligned}\Delta G_f &= -RT \ln K_{\text{chem},N} \\ &= -RT \ln(\overline{EM}^{N-1} K_1^N) \\ &= RT \ln \overline{EM} - N\,RT(\ln \overline{EM} + \ln K_1) \end{aligned} \quad (10)$$

The gradient of the line for the linear oligomers gives $\overline{EM} = 0.034$ M, which is in excellent agreement with the average effective molarity of *l*-P′6·T6 determined using eq 9 ($\overline{EM}_6 = 0.032$ M). For the cyclic oligomers, the linear region of the plot, for $N = 2-6$, gives $\overline{EM} = 730$ M, which is close to the geometric average of EM_3-EM_6 (700 M), confirming the high effective molarities for $N = 3-6$.

A key assumption underlying the analysis presented here is that the denaturation titrations (Figure 4) can be analyzed as all-or-nothing two-state equilibria, so that each denaturation curve can be fitted by eq 3 using just three free parameters (A_0, A_f, and K_{dn}). It would be impossible to analyze these titrations without making this assumption because a full set of partially bound species would lead to too many free variables. This assumption is supported by the isosbestic nature of the UV/vis titrations (Figure 4) and by the good fits to the calculated binding curves. Knowledge of the effective molarities (Table 1) allows us to check whether this two-state assumption is consistent with the results by calculating speciation curves for the denaturation reactions (see the Supporting Information for details). These calculations confirm that denaturation is essentially a two-state process for both linear and cyclic oligomer complexes; for example, the speciation curves for denaturation of *c*-P6·T6 are plotted in

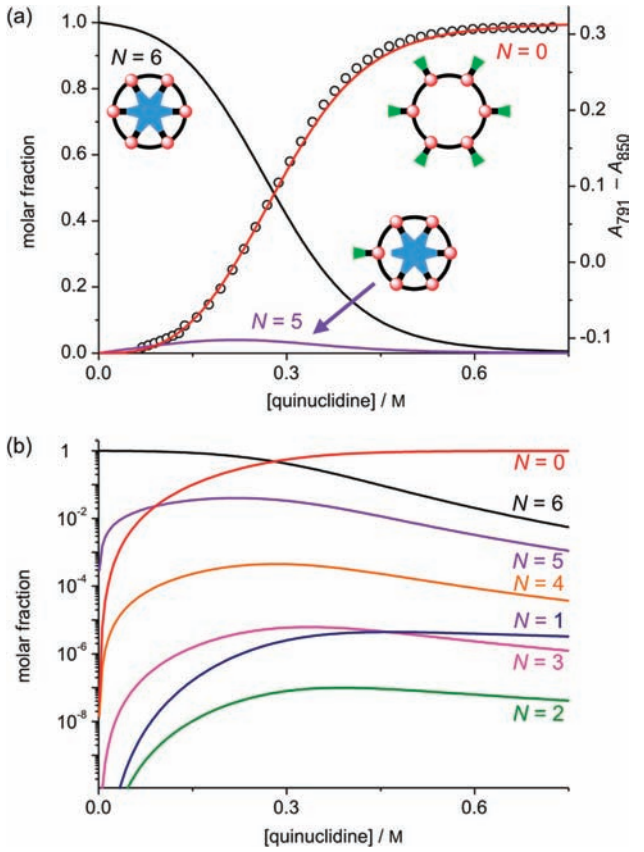

Figure 7. Speciation profiles for denaturation of *c*-P6·T6 (2 μM) with quinuclidine: (a) molar fraction of species in the course of the titration (N is the number of template-bound binding sites of the nanoring) and measured difference in absorption (791−850 nm) in the course of the titration; (b) same speciation profile on a logarithmic scale. The concentrations of the species with N = 1−4 are too low to be visible on the linear scale of plot a.

Figure 7. The two most abundant species in the course of the titration are the fully template-bound nanoring complex (N = 6) and the quinuclidine-saturated nanoring (N = 0). The only other species that reaches noticeable concentrations is the five-pyridyl-bound complex (N = 5; peak mole fraction 0.04). Figure 7b shows that other partially denatured species with one to four coordinated pyridines (N = 1−4) are formed in very low concentrations. The presence of two dominant species in this equilibrium, accounting for 96% of the material, justifies the use of an all-or-nothing binding model and illustrates the high cooperativity of the binding process.

CONCLUSIONS

This work demonstrates that rigid preorganized shape-complementary multivalent host−guest systems can exhibit high effective molarities (up to 10^3 M) and very high association constants (up to 10^{36} M^{-1}). An effective molarity of 10^3 M matches the upper limit to EM estimated from the entropy of the zinc−porphyrin pyridine interaction,[3c,17] but systems exhibiting such high effective molarities have not been previously reported. The effective molarities reported here are statistically corrected. Other authors often use the symbol EM to indicate the product of the microscopic effective molarity multiplied by the statistical factor of the cyclization process;[3a] if we used this definition, our values of EM would be larger by about a factor of 3.

The highly cooperative nature of the binding of cyclic porphyrin hexamer *c*-P6 with hexadentate ligand T6 is evident from the denaturation of this complex with quinuclidine, both from the sigmoidal shape of the denaturation curve (Figure 7a) and from the low concentrations of partially bound intermediate complexes seen in the speciation profiles (Figure 7b). The strong chelate cooperativity is caused both by the high effective molarity and by the high single-site binding constant (K_1).[2,3a] For *c*-P6·T6, $K_1(\overline{EM}) = 7.8 \times 10^5$, which means that all the intramolecular coordination steps in Figure 2a are extremely favorable.

All the effective molarities reported here are thermodynamic values for equilibrium processes. Ligand T6 is also a very effective template for directing the synthesis of *c*-P6, which implies that it will be interesting to compare stepwise kinetic and thermodynamic effective molarities in this system.

ASSOCIATED CONTENT

Supporting Information. Synthesis and characterization of new compounds, UV/vis titrations and binding data for reference compounds and for the formation of linear oligomer complexes, derivation of binding equations, error analysis and calculation of statistical factors, calculation of speciation profiles, and complete ref 26. This material is available free of charge via the Internet at http://pubs.acs.org.

AUTHOR INFORMATION

Corresponding Author
harry.anderson@chem.ox.ac.uk

ACKNOWLEDGMENT

We thank the European Commission for support (through THREADMILL, Grant MRTN-CT-2006-036040, studentship to J.K.S., and Grant MEIF-CT-2006-041629, fellowship to M.P.) and the EPSRC Mass Spectrometry Service (Swansea) for the mass spectra. We are grateful to Melanie C. O'Sullivan for valuable discussion.

REFERENCES

(1) (a) Page, M. I.; Jenks, W. P. *Proc. Natl. Acad. Sci. U.S.A.* **1971**, *68*, 1678–1683. (b) Page, M. I. *Angew. Chem., Int. Ed. Engl.* **1977**, *16*, 449–459.

(2) Hunter, C. A.; Anderson, H. L. *Angew. Chem., Int. Ed.* **2009**, *48*, 7488–7499.

(3) (a) Ercolani, G.; Schiaffino, L. *Angew. Chem., Int. Ed.* **2011**, *50*, 1762–1768. (b) Ercolani, G. *J. Phys. Chem. B* **2003**, *107*, 5052–5057. (c) Ercolani, G. *Struct. Bonding (Berlin)* **2006**, *121*, 167–215.

(4) In the situation shown in Figure 1, there is no symmetry in the host or the guest, so no statistical factors are required, but often statistical factors need to be included in the calculation of EM to account for the different degeneracies of the species involved in the equilibrium.

(5) (a) Ercolani, G.; Mandolini, L.; Mencarelli, P.; Roelens, S. *J. Am. Chem. Soc.* **1993**, *115*, 3901–3908. (b) Ercolani, G.; Di Stefano, S. *J. Phys. Chem. B* **2008**, *112*, 4662–4665.

(6) Huskens, J.; Mulder, A.; Auletta, T.; Nijhuis, C. A.; Ludden, M. J. W.; Reinhoudt, D. N. *J. Am. Chem. Soc.* **2004**, *126*, 6784–6797.

(7) Krishnamurthy, V. M.; Semetey, V.; Bracher, P. J.; Shen, N.; Whitesides, G. M. *J. Am. Chem. Soc.* **2007**, *129*, 1312–1320.

(8) de Greef, T. F. A.; Ercolani, G.; Ligthart, G. B. W. L.; Meijer, E. W.; Sijbesma, R. P. *J. Am. Chem. Soc.* **2008**, *130*, 13755–13764.

(9) De Greef, T. F. A.; Smulders, M. M. J.; Wolffs, M.; Schenning, A. P. H. J.; Sijbesma, R. P.; Meijer, E. W. *Chem. Rev.* **2009**, *109*, 5687–5754.
(10) Misuraca, M. C.; Grecu, T.; Freixa, Z.; Garavini, V.; Hunter, C. A.; van Leeuwen, P. W. N. M.; Segarra-Maset, M. D.; Turega, S. M. *J. Org. Chem.* **2011**, *76*, 2723–2732.
(11) (a) Cram, D. J.; Lein, G. M.; Kaneda, T.; Helgeson, R. C.; Knobler, C. B.; Maverick, E.; Trueblood, K. N. *J. Am. Chem. Soc.* **1981**, *103*, 6822–6232. (b) Cram, D. J. *Angew. Chem., Int. Ed. Engl.* **1986**, *25*, 1039–1057.
(12) (a) van Eerden, J.; Grootenhuis, P. D. J.; Dijkstra, P. J.; van Staveren, C. J.; Harkema, S.; Reinhoudt, D. N. *J. Org. Chem.* **1986**, *51*, 3918–3920. (b) Hua, Y.; Ramabhadran, R. O.; Karty, J. A.; Raghavachari, K.; Flood, A. H. *Chem. Commun.* **2011**, *47*, 5979–5981.
(13) Zhong, Z.; Li, X.; Zhao, Y. *J. Am. Chem. Soc.* **2011**, *133*, 8862–8865.
(14) (a) Hancock, R. D.; Marsicano, F. *J. Chem. Soc., Dalton Trans.* **1976**, 1096–1098. (b) Meyers, R. T. *Inorg. Chem.* **1978**, *17*, 952–958.
(15) Watson, J. L.; Whitesides, G. M. *J. Org. Chem.* **1993**, *58*, 642–647.
(16) Anderson, H. L. *Inorg. Chem.* **1994**, *33*, 972–981.
(17) Anderson, H. L.; Anderson, S.; Sanders, J. K. M. *J. Chem. Soc., Perkin Trans. 1* **1995**, 2231–2245.
(18) (a) Hunter, C. A.; Misuraca, M. C.; Turega, S. M. *J. Am. Chem. Soc.* **2011**, *133*, 582–594. (b) Hunter, C. A.; Ihekwaba, N.; Misuraca, M. C.; Segarra-Maset, M. D.; Turega, S. M. *Chem. Commun.* **2009**, 3964–3966. (c) Chekmeneva, E.; Hunter, C. A.; Packer, M. J.; Turega *J. Am. Chem. Soc.* **2008**, *130*, 17718–17725. (d) Bernad, P. L.; Guerin, A. J.; Haycock, R. A.; Heath, S. L.; Hunter, C. A.; Raposo, C.; Rotger, C.; Sarson, L. D.; Sutton, L. R. *New J. Chem.* **2008**, *32*, 525–532.
(19) (a) González-Álvarez, A.; Frontera, A.; Ballester, P. *J. Phys. Chem. B* **2009**, *115*, 11479–11489. (b) Ballester, P.; Oliva, A. I.; Costa, A.; Deyà, P. M.; Frontera, A.; Gomila, R. M.; Hunter, C. A. *J. Am. Chem. Soc.* **2006**, *128*, 5560–5569.
(20) Oshovsky, G. V.; Reinhoudt, D. N.; Verboom, W. *J. Org. Chem.* **2006**, *71*, 7441–7448.
(21) Ikeda, C.; Tanaka, Y.; Fujihara, T.; Ishii, Y.; Ushiyama, T.; Yamamoto, K.; Yoshioka, N.; Inoue, H. *Inorg. Chem.* **2001**, *40*, 3395–3405.
(22) Kassianidis, E.; Pearson, R. J.; Philp, D. *Chem.—Eur. J.* **2006**, *12*, 8798–8812.
(23) Hammerstein, A. F.; Shin, S.-H.; Bayley, H. *Angew. Chem., Int. Ed.* **2010**, *49*, 5085–5090.
(24) In this paper we consider only thermodynamic effective molarities for equilibrium processes. It is well known that kinetic effective molarities can have higher values; e.g., see: Cacciapaglia, R.; Di Stefano, S.; Mandolini, L. *Acc. Chem. Res.* **2004**, *37*, 113–122.
(25) Hoffmann, M.; Kärnbratt, J.; Chang, M.-H.; Herz, L. M.; Albinsson, B.; Anderson, H. L. *Angew. Chem., Int. Ed.* **2008**, *47*, 4993–4996.
(26) The crystal structure of *c*-P6·T6 shows that the *c*-P6 nanoring is too large for a perfect fit to the T6 ligand by a factor of 2.5%. This crystal structure also shows that the geometry of the Zn−pyridine coordination sphere in *c*-P6·T6 is normal, with no signs of strain-induced distortion; see: Sprafke, J. K.; et al. *J. Am. Chem. Soc.* **2011**, *133*, 17262–17273.
(27) In a preliminary study[25] we determined the stability of the complex *c*-P′6·T6 with octyloxy side chains and reported $K_f = 6.6 \times 10^{38}$ M, whereas here we report $K_f = 1.2 \times 10^{36}$ M for *c*-P6·T6 with *tert*-butyl side chains. The difference between these values originates largely from the difference in side chains. The statistically corrected geometrically averaged effective molarity determined for *c*-P′6·T6 was log $\overline{EM}_6$ = 2.0, which is similar to the value of log $\overline{EM}_6$ = 2.1 reported here for *c*-P6·T6.
(28) (a) Dilthey, W.; Quint, F. *J. Prakt. Chem.* **1930**, *128*, 139–149. (b) Dilthey, W.; Hurtig *Chem. Ber.* **1934**, *67B*, 2004–2007. (c) Fieser, L. F. *Organic Syntheses*; Wiley & Sons: New York, 1973; Collect. Vol. V, p 604. (d) Shen, X.; Ho, D. M.; Pascal, R. A. *J. Am. Chem. Soc.* **2004**, *126*, 5798–5805. (e) Sauriat-Dorizon, H.; Maris, T.; Wuest, J. D. *J. Org. Chem.* **2003**, *68*, 240–246.
(29) Drobizhev, M.; Stepanenko, Y.; Rebane, A.; Wilson, C. J.; Screen, T. E. O.; Anderson, H. L. *J. Am. Chem. Soc.* **2006**, *128*, 12432–12433.
(30) K_Q is the binding constant of quinuclidine per porphyrin unit; it is not a microscopic binding constant. K_Q is measured for a porphyrin monomer, *l*-P′1, in the case of the linear oligomers, because the longer linear oligomers aggregate in the absence of pyridine even at micromolar concentrations. K_Q can be measured directly for *c*-P6 because this cyclic oligomer does not aggregate significantly at low concentrations. The difference in K_Q of about a factor of 3 appears to be a consequence of the inductive effect of the alkoxy groups used to solubilize the linear oligomers; a similar difference is also seen between the K_1 values for the two types of oligomers.
(31) Winters, M. U.; Kärnbratt, J.; Eng, M.; Wilson, C. J.; Anderson, H. L.; Albinsson, B. *J. Phys. Chem. C* **2007**, *111*, 7192–7199.
(32) Sprafke, J. K.; Stranks, S. D.; Warner, J. H.; Nicholas, R. J.; Anderson, H. L. *Angew. Chem., Int. Ed.* **2011**, *50*, 2313–2316.
(33) (a) Benson, S. W. *J. Am. Chem. Soc.* **1958**, *80*, 5151–5154. (b) Bailey, W. F.; Monahen, A. S. *J. Chem. Educ.* **1978**, *55*, 489–493.
(34) Ercolani, G.; Piguet, C.; Borkovec, M.; Hamacek, J. *J. Phys. Chem. B* **2007**, *111*, 12195–12203.
(35) Note that a chelate effect requires more than one point of interaction; no effective molarity exists for $N = 1$, and eqs 7−9 are not defined for EM_1.
(36) Lovett, J. E.; Hoffmann, M.; Cnossen, A.; Shutter, A. T. J.; Hogben, H. J.; Warren, J. E.; Pascu, S. I.; Kay, C. W. M.; Timmel, C. R.; Anderson, H. L. *J. Am. Chem. Soc.* **2009**, *131*, 13852–13859.
(37) Saywell, A; Sprafke, J. K.; Esdaile, L. J.; Britton, A. J.; Rienzo, A.; Anderson, H. L.; O'Shea, J. N.; Beton, P. H. *Angew. Chem., Int. Ed.* **2010**, *49*, 9136–9139.
(38) (a) Ercolani, G. *Org. Lett.* **2005**, *7*, 803–805. (b) Shinkai, S.; Sugasaki, A.; Ikeda, M.; Takeuchi, M. *Acc. Chem. Res.* **2001**, *34*, 494–503. (c) Wilson, G. S.; Anderson, H. L. *Chem. Commun.* **1999**, 1539–1540.